

Design Formulas for the Leakage Inductance of Toroidal Distribution Transformers

Iván Hernández, *Student Member, IEEE*, Francisco de León, *Senior Member, IEEE*, and Pablo Gómez, *Member, IEEE*

Abstract—In this paper, design formulas for the calculation of the leakage inductance of toroidal transformers are presented. The formulas are obtained from the analytical integration of the stored energy. The formulas are sufficiently simple and accurate to be introduced in the loop of a design program avoiding expensive finite element simulations. It is found that toroidal transformers naturally produce the minimum leakage inductance possible for medium-voltage power transformers. To limit the short-circuit currents in power and distribution systems, a larger than the minimum leakage inductance is often required. This paper presents two methodologies to increase the leakage inductance of toroidal distribution transformers: selectively enlarging the inter-winding spacing and inserting a piece of ferromagnetic material in the leakage flux region between the windings. Extensive validation with 2D and 3D finite element simulations is performed. Additionally, experimental verification of both formulas and numerical simulations was carried out comparing the calculations against measurements on prototypes.

Index Terms—Finite-element method, leakage inductance, toroidal transformers.

I. INTRODUCTION

FARADAY in 1831 built the first transformer in a toroidal core [1]; see Fig. 1. The first industrial grade transformer, the one of the Ganz factory in Budapest of 1885, was also wound on a toroidal core [2] (see Fig. 2). Currently, however, toroidal transformers are not widely used for transmission and distribution of bulk power. There are two basic arrangements used to build the iron cores of medium and large transformers [3]–[6]: 1) core type where the cores are assembled by stacking laminations and sliding premade windings and 2) shell type, where a continuously wound core is cut and wrapped around the windings a few laminations at a time. In both arrangements, the finished core has air gaps that increase the magnetizing current and the no-load losses.

Toroidal transformers have found modern applications in the low-voltage low power of many power supplies for electronic



Fig. 1. Photo of Faraday's original transformer [1].

equipment, avionics, and audio systems [7], [8]. A very limited amount of published material exists in the IEEE related to toroidal transformers for power conversion applications; see [9]–[11]. There are not any papers published related to mid- or high-voltage toroidal transformers intended for use at utility voltages. Transformers wound on nongapped toroidal cores using grain-oriented silicon (Si) steel are more efficient, smaller, cooler, and emit reduced acoustic and electromagnetic noise when compared with standard transformer constructions. To extrapolate these advantages to distribution transformers, an effort is being made now, as part of a U.S. Department of Energy funded project, to produce toroidal transformers suitable for power distribution system applications. Although toroidal transformers have many advantages over traditional constructions, there are also a few disadvantages that need to be overcome before widespread adoption of toroidal transformers is possible. Most important, there is no published experience in the industry when it comes to designing and building toroidal transformers suitable for operation at medium and high voltage. Unresolved issues with toroidal transformer design and manufacturing include matching the leakage impedance specification, limiting inrush currents, designing and constructing to withstand short-circuit currents, the study of electromagnetic transients (impulse test), design for cost optimization, and the ability to pass industry-standard acceptance tests. This paper is part of a series describing the solutions to those issues via electromagnetic design, design verification, building prototypes, performance verification, and observation of prototypes installed on a utility distribution system. In low-voltage, low-power applications, the leakage inductance can be minimized using planar transformers or highly interleaved windings. For high-power, medium-voltage transformers, the leakage inductance of toroids is the minimum achievable. The reason for this is the closed concentric geometry. The first winding

Manuscript received June 17, 2010; revised March 08, 2011; accepted May 10, 2011. Date of publication June 28, 2011; date of current version October 07, 2011. This work was supported by the U.S. Department of Energy under Grant DEOE0000072. Paper no. TPWRD-00457-2010.

I. Hernández is with the CINVESTAV Guadalajara, Jalisco 45015, México (e-mail: ihernand@gdl.cinvestav.mx).

F. de León is with the Department of Electrical and Computer Engineering of Polytechnic Institute of New York University, Brooklyn, NY 11201 USA (e-mail: fdeleon@poly.edu).

P. Gómez is with the Electrical Engineering Department, SEPI-ESIME Zacatenco, Instituto Politécnico Nacional (IPN), Mexico City 07738, Mexico (e-mail: pgomez@ipn.mx).

Color versions of one or more of the figures in this paper are available online at <http://ieeexplore.ieee.org>.

Digital Object Identifier 10.1109/TPWRD.2011.2157536



Fig. 2. Drawing of the Ganz factory transformer [2].

completely covers the core and subsequent windings cover the internal windings. There are no yokes where the flux could escape to the air. Therefore, the electromagnetic coupling is maximized, while the leakage and stray fields are minimized. The small regulation characteristic that can be obtained with toroidal transformers by minimizing the leakage impedance is desirable for many applications. However, in a power system, the transformers' leakage impedance is one of the important components used for limiting the short-circuit currents. Consequently, a larger than natural leakage inductance may be required for a toroidal transformer.

A contribution of this paper is to propose two methods to increase the leakage inductance of toroidal transformers: 1) enlarging the spacing between primary and secondary windings and 2) inserting high permeability materials between primary and secondary windings.

Another contribution of this paper is the derivation of equations suitable for implementation in a design program for the calculation of the leakage inductance of toroidal transformers. The final expressions are numerically very efficient and sufficiently accurate for practical design work. Validation against a large number of finite-element simulations in 2-D and 3-D covering distribution transformers of 25, 37.5, 50, and 75 kVA was performed.

II. DISTRIBUTION OF THE LEAKAGE FIELD

Coherent with the standardized method to measure the leakage inductance, for its computation, one must simulate the short-circuit test. In other words, force $N_1 I_1 = N_2 I_2$, eliminating the magnetizing current. Fig. 3(a) shows an axisymmetric view of the distribution of the magnetic-field strength in a toroidal transformer during a short-circuit test. Five distinct sections having different field distribution characteristics can be identified:

- 1) vertical internal part of the windings;
- 2) vertical external part of the windings;
- 3) top and bottom horizontal parts;
- 4) internal corners;

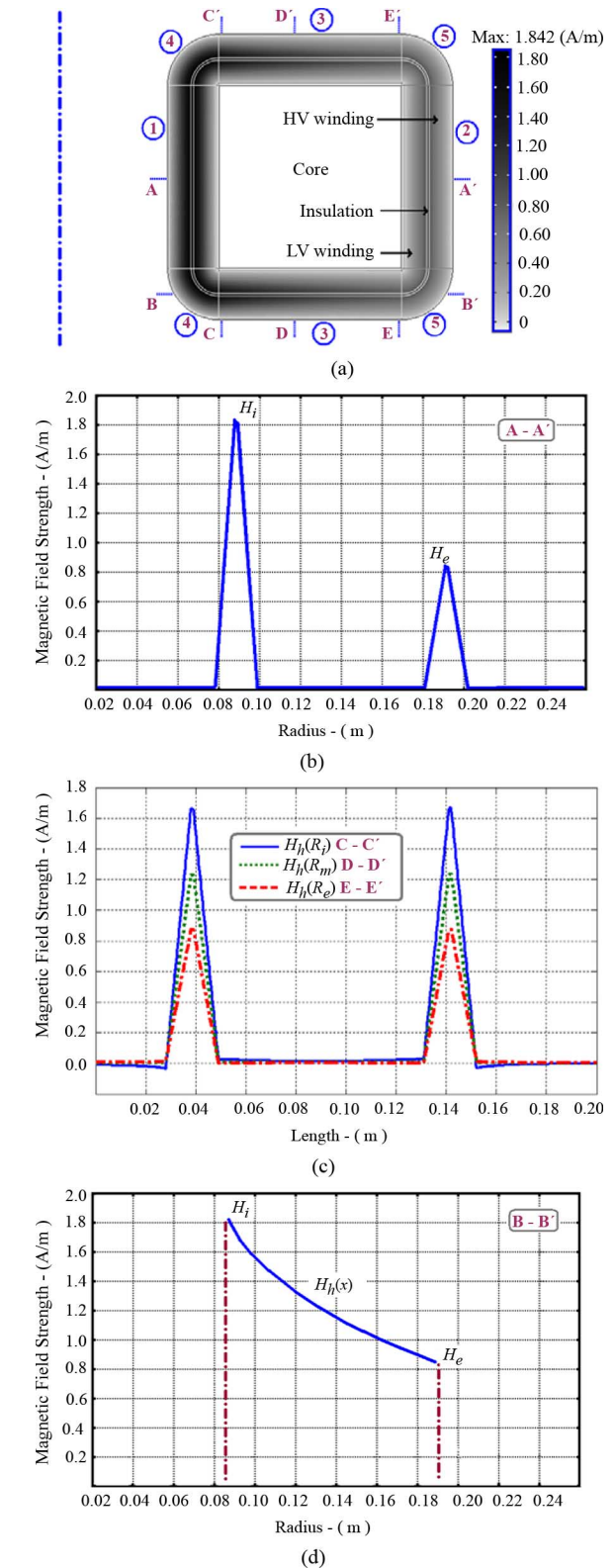


Fig. 3. Distribution of the magnetic-field strength in the toroidal transformer: (a) Axisymmetric view. (b) Radial distribution of the magnetic field on the vertical sections. (c) Magnetic-field strength on the horizontal sections at three positions. (d) Radial variation of the field at the insulation of the horizontal parts.

- 5) external corners.

One can distinguish three subregions: two corresponding to the two windings and one for the insulation between them

in each of the five regions. Fig. 3(b) shows the magnetic-field strength on the vertical part of the windings along the line A-A'. One can see that the magnetic flux in the vertical direction almost follows the trapezoidal distribution characteristic of traditional transformer designs. In addition, note that the magnetic-field strength is independent of the vertical position.

The top and bottom sections, regions 3 of Fig. 3(a), have identical magnetic-field distributions as shown in Fig. 3(c). Note, however, that while the vertical variation of the field follows the trapezoidal distribution, the field strength reduces in inverse proportion with the distance to the axis; see Fig. 3(d).

The leakage inductance of the toroidal transformer can be obtained through closed-form volumetric integration of the distribution of the magnetic energy stored as follows:

$$\begin{aligned} L_{\text{leak}} &= \frac{2W_{\text{stored}}}{I^2} \\ &= \frac{2}{I^2} \int_V \frac{H \cdot B}{2} dV = \frac{\mu_0}{I^2} \int_V |H|^2 dV. \end{aligned} \quad (1)$$

It is noticed that the different components of the leakage inductance can be obtained by analyzing the distribution of the magnetic-field strength H at each section. Two main assumptions are made regarding the distribution of the magnetic-field strength as follows.

- The radial distribution (around the toroidal circumference) is considered constant (axisymmetric model).
- The distribution of H transversal to the windings is considered as follows: it rises linearly in one winding, varies inversely with x in the insulation between windings, and decays linearly in the opposite winding. This type of distribution can be described by the following expression:

$$H = \begin{cases} H_{\text{peak}} \left(\frac{x}{a} \right), & 0 \leq x \leq a \\ H(x), & a \leq x \leq a+g \\ H_{\text{peak}} \left(1 - \frac{x-a-g}{b} \right), & a+g \leq x \leq a+g+b \end{cases} \quad (2)$$

where H_{peak} is the maximum value of the magnetic-field strength; in this paper, H_{peak} is identified in five ways depending on the section being considered: H_i , H_e (internal and external vertical sections of the winding, respectively); $H_{gi}(x)$, $H_{ge}(x)$ correspond to the internal and external spaces between the windings (i.e., insulation); and $H_h(x)$ (horizontal sections of the winding); while a , b , and g correspond to the thickness of the high-voltage (HV) winding, low-voltage (LV) winding, and interwinding insulation, respectively (as indicated in Fig. 4).

III. DESIGN FORMULAS FOR THE LEAKAGE INDUCTANCE

From the identification of the five different sections, the total leakage inductance of the winding can be computed as

$$L_{\text{leak}} = L_{\text{leak},1} + L_{\text{leak},2} + 2L_{\text{leak},3} + 2L_{\text{leak},4} + 2L_{\text{leak},5} \quad (3)$$

where $L_{\text{leak},i}$ corresponds to the leakage inductance component of the i th section of the winding (for $i = 1, 2, 3, 4, 5$). Expressions for each section will be obtained as shown (using the Cartesian coordinate system).

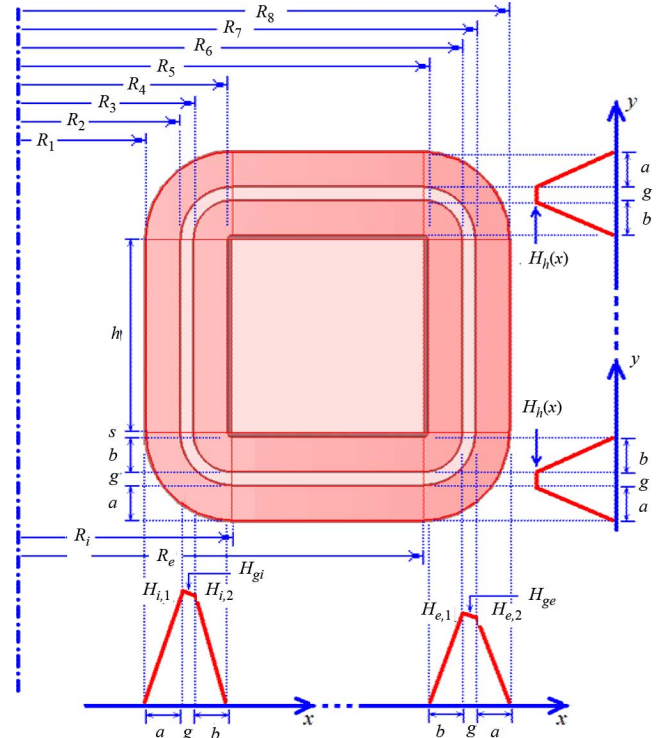


Fig. 4. Main geometrical data of a toroidal distribution transformer.

A. Vertical Parts (Sections I and II)

In Sections I and II (internal and external vertical parts of the winding, respectively), the peak values of $H(H_i, H_e, H_{gi}, H_{ge})$ are shown in Fig. 4. These peaks can be computed from Ampere's Law as follows:

$$\begin{aligned} H_{i,1} &= \frac{NI}{2\pi R_2}; H_{gi}(x) = \frac{NI}{2\pi(R_2 + x)}; \\ H_{i,2} &= \frac{NI}{2\pi R_3}; \end{aligned} \quad (4a)$$

$$\begin{aligned} H_{e,1} &= \frac{NI}{2\pi R_6}; H_{ge}(x) = \frac{NI}{2\pi(R_6 + x)}; \\ H_{e,2} &= \frac{NI}{2\pi R_7}; \end{aligned} \quad (4b)$$

where N is the number of turns of the exciting winding; I is the current; R_2 and R_6 are the internal radii of the insulation for the vertical regions 1 and 2, respectively; and R_3 and R_7 are the internal radii of the external winding for regions 1 and 2. The reduction of the magnetic-field strength between the windings, from H_{gi} to H_{ge} as $1/x$ is considered. When the insulation between windings is small, we can assume that H has a trapezoidal distribution. In [12], we have computed that 1 mm of insulation between windings is enough to produce transformers class 95-kV BIL.

Combining (1) and (4), the leakage inductance of Section I is computed from

$$L_{\text{leak},1} = \frac{2\pi\mu_0 h}{I^2} \left[R_{m1} \int_0^a \left| H_{i,1} \left(\frac{x}{a} \right) \right|^2 dx \right]$$

$$\begin{aligned}
& +R_{m2} \int_a^{a+g} |H_{gi}|^2 dx \\
& +R_{m3} \int_{a+g}^{a+g+b} \left| H_{i,2} \left(1 - \frac{x-a-g}{b} \right) \right|^2 dx \Big] \quad (5)
\end{aligned}$$

where h is the height of the toroid; R_{m1} , R_{m2} , and R_{m3} correspond to mean radii of the HV winding, insulation, and LV winding, respectively, and computed, in general, as

$$R_{mj} = \frac{(R_j + R_{j+1})}{2}. \quad (6)$$

Substituting (4a) into (5) and performing the integral, one obtains

$$\begin{aligned}
L_{\text{leak},1} &= \frac{N^2 \mu_0 h}{2\pi} \left[\left(\frac{R_{m1}}{R_2^2} \right) \frac{a}{3} + \left(\frac{R_{m2}}{R_2 R_3} \right) \frac{g}{2} + \left(\frac{R_{m3}}{R_3^2} \right) \frac{b}{3} \right]. \quad (7)
\end{aligned}$$

The leakage inductance for Section II is computed in a similar manner as

$$\begin{aligned}
L_{\text{leak},2} &= \frac{N^2 \mu_0 h}{2\pi} \left[\left(\frac{R_{m5}}{R_6^2} \right) \frac{a}{3} + \left(\frac{R_{m6}}{R_6 R_7} \right) \frac{g}{2} + \left(\frac{R_{m7}}{R_7^2} \right) \frac{b}{3} \right]. \quad (8)
\end{aligned}$$

B. Horizontal Parts (Section III)

The top and bottom parts have the same field distribution; see Fig. 3(c). The value of H at the interwinding insulation is computed from Ampere's Law as follows:

$$H_h(x)at = \frac{NI}{2\pi x}. \quad (9)$$

The radial distance on the x -axis can take values from $R_i \leq x \leq R_e$, where R_i and R_e are the internal and external radii of the toroid, respectively. Thus, the leakage inductance of the horizontal sections is obtained from (10), shown at the bottom of the page. R_{mh} is the mean radius of the horizontal sections, given by

$$R_{mh} = \frac{(R_i + R_e)}{2}. \quad (11)$$

Substituting (9) in (10), performing the integral, and using (11), we obtain

$$L_{\text{leak},3} = \frac{N^2 \mu_0 (R_e^2 - R_i^2)}{2\pi R_e R_i} \left(\frac{b}{3} + g + \frac{a}{3} \right). \quad (12)$$

C. Corners (Sections IV and V)

For the corners, the same peak values for the magnetic field defined for the internal H_i and external H_e vertical parts are considered as given by (4a) and (4b). The trapezoidal distribution of H is around the corner, so it was necessary to perform the integral around its periphery denoted by φ (from 0 to $\pi/2$); the leakage inductance for the internal corners is obtained from (13), shown at the bottom of the page.

Solving (13), it follows that:

$$L_{\text{leak},4} = \frac{N^2 \mu_0}{4\pi R_2^2} \left(\frac{R_{m1} t_1 a}{6} + R_{m2} t_2 g + \frac{R_{m3} t_3 b}{6} \right) \quad (14)$$

where

$$t_1 = 3a + 4(s + b + g) \quad (15a)$$

$$t_2 = g + 2(s + b) \quad (15b)$$

$$t_3 = 3b + 4s. \quad (15c)$$

$$\begin{aligned}
L_{\text{leak},3} &= \frac{2\pi \mu_0 R_{mh}}{I^2} \left\{ \int_{R_i}^{R_e} \left[\int_0^b \left| H_h \left(\frac{y}{b} \right) \right|^2 dx \right. \right. \\
& \quad + \int_b^{b+g} |H_h|^2 dx \\
& \quad \left. \left. + \int_{b+g}^{b+g+a} \left| H_h \left(1 - \frac{y-b-g}{a} \right) \right|^2 dx \right] dy \right\}. \quad (10)
\end{aligned}$$

$$\begin{aligned}
L_{\text{leak},4} &= \frac{2\pi \mu_0}{I^2} \left\{ \int_0^{\pi/2} \left[R_{m1} \int_0^a \left| H_{i,1} \left(\frac{x}{a} \right) \right|^2 x dx \right. \right. \\
& \quad + R_{m2} \int_a^{a+g} |H_{gi}|^2 x dx \\
& \quad \left. \left. + R_{m3} \int_{a+g}^{a+g+b} \left| H_{i,2} \left(1 - \frac{x-a-g}{b} \right) \right|^2 x dx \right] d\varphi \right\} \quad (13)
\end{aligned}$$

TABLE I
COEFFICIENTS FOR THE DIFFERENT COMPONENTS OF THE LEAKAGE
INDUCTANCE FORMULA (17)

Section	Coefficient			
	η_i	α_i	ϕ_i	β_i
1	h	$\frac{R_{m1}}{3R_2^2}$	$\frac{R_{m2}}{2R_2R_3}$	$\frac{R_{m3}}{3R_3^2}$
2	h	$\frac{R_{m7}}{3R_7^2}$	$\frac{R_{m6}}{2R_6R_7}$	$\frac{R_{m5}}{3R_6^2}$
3	$\frac{R_e^2 - R_i^2}{R_e R_i}$	$\frac{1}{3}$	1	$\frac{1}{3}$
4	$\frac{1}{2R_2^2}$	$\frac{R_{m1}t_1}{6}$	$R_{m2}t_2$	$\frac{R_{m3}t_3}{6}$
5	$\frac{1}{2R_6^2}$	$\frac{R_{m7}t_1}{6}$	$R_{m6}t_2$	$\frac{R_{m5}t_3}{6}$

Similarly, the leakage inductance for the external corners is computed as

$$L_{,5} = \frac{N^2 \mu_0}{4\pi R_6^2} \left(\frac{R_{m5}t_3b}{6} + R_{m6}t_2g + \frac{R_{m7}t_1a}{6} \right). \quad (16)$$

D. Generalized Expression

One can appreciate that (7), (8), (12), (14), and (16) have a similar form. Therefore, a generalized expression for the calculation of the contribution to the leakage inductance of each section can be obtained as follows:

$$L_{\text{leak},i} = \frac{N^2 \mu_0}{2\pi} \eta_i (\alpha_i a + \phi_i g + \beta_i b). \quad (17)$$

The coefficients for the different sections are given in Table I. The total leakage inductance is computed from (3).

IV. TEST CASES

Table II shows the design parameters of a set of toroidal distribution transformers used to demonstrate the applicability of the methods and the accuracy of the formulas. We have selected the standardized sizes for distribution transformers per [13]. The leakage inductance reference values have been computed with 3-D finite-element simulations using the commercially available software (COMSOL Multiphysics) [14].

The FEM simulations performed solve for the magnetostatic formulation. All materials are considered as being isotropic; we used copper windings and electrical steel M4 (0.28 mm) for the main core considering its B-H curve as provided by the manufacturer.

In the simulations, the toroid was enclosed by a tank represented by a rectangle in the axisymmetric 2-D case and by a cylinder in the 3-D case. Magnetic insulation was applied to the boundaries of the tank walls. For the 2-D simulations, about 40 000 triangular elements were necessary, consuming about 2 GB of random-access memory (RAM). For the 3-D simulations, about 400 000 tetrahedrons were employed, consuming 9-GB

TABLE II
DESIGN PARAMETERS FOR SINGLE-PHASE TOROIDAL TRANSFORMERS

	25 kVA	37.5 kVA	50 kVA	75 kVA
HV-(kV)	13.80	13.80	13.80	13.80
LV-(kV)	0.12	0.12	0.12	0.12
B_m (T)	1.70	1.70	1.70	1.70
f (Hz)	60.00	60.00	60.00	60.00
N_p	4715	4370	4370	3335
R_1 (mm)	100.00	101.50	110.50	121.50
R_e (mm)	180.00	185.50	194.50	217.50
h (mm)	80.00	84.00	84.00	96.00
a (mm)	10.24	12.64	17.39	17.90
b (mm)	10.41	10.41	11.68	20.81
g (mm)	1.00	1.00	1.00	1.00
s (mm)	0.50	0.50	0.50	0.50

B_m is the magnetic flux density average in the core, f is the operation frequency, N_p is the number of turns of the HV side.

TABLE III
PARAMETERS COMPUTED FOR SINGLE-PHASE TOROIDAL TRANSFORMERS

	Leakage Inductance (H)		Leakage Reactance (%)		%
	FEM	Formula	FEM	Formula	
25 kVA	0.1050	0.1079	0.5198	0.5339	2.76
37.5 kVA	0.1011	0.1041	0.7508	0.7724	2.99
50 kVA	0.1200	0.1236	1.1879	1.2234	3.01
75 kVA	0.1086	0.1114	1.6121	1.6544	2.86

The computed values were referred to the HV winding.

TABLE IV
IMPEDANCE DATA FOR THE SINGLE-PHASE TRANSFORMERS FROM [13]

kVA	Suggested X/R Ratio for Calculation	Normal Range of Percent Impedance (% Z)
1-phase		
25.0	1.1	1.2-6.0
37.5	1.4	1.2-6.5
50.0	1.6	1.2-6.4
75.0	1.8	1.2-6.6

RAM. The axisymmetric 2-D and 3-D simulation results were almost identical. Therefore, we conclude, as expected from a symmetrical construction, that to compute the leakage inductance, 2-D axisymmetric modeling is sufficient.

Table III shows the values of leakage inductances and reactances in percent that can be achieved with toroidal transformers. The inductive values are referred to the HV winding. From Table III, one can appreciate that the results are in good agreement, with maximum differences of 3%.

Table IV shows the leakage impedance values recommended by the IEEE Standard 242-1986 [13] for the calculation of short-circuit currents. It can be noticed that the reactance in percent of toroidal transformers may be substantially smaller than that of conventional transformers. Therefore, larger short-circuit currents can be expected. Although small regulation is, in general, a desirable characteristic for a transformer, for some applications, the larger short-circuit currents that occur may not be acceptable. In the next section, two methods to increase the leakage inductance are proposed.

V. METHODOLOGIES FOR INCREASING THE LEAKAGE INDUCTANCE OF TOROIDAL TRANSFORMERS

A. Increasing Interwinding Spacing

One can perceive from Tables III and IV that the leakage inductance of a 25-kVA toroidal transformer may be as small as half of what is specified in the standard [12].

From the expressions obtained in Section III and their analogy with the technology of traditional transformer constructions, it can be inferred that increasing the spacing between windings will increase the leakage inductance. This is a technique known to designers and manufacturers of traditional transformer constructions. It is possible to identify in (7), (8), (12), (14) and (16) the middle term as the inductance corresponding to leakage flux in the insulation (or air). To build toroidal transformers, the internal space at the center of the toroid must be large enough for the winding machine to pass. Therefore, only the top, bottom, and external regions can be used in practice to increase the leakage path. Furthermore, when considering manufacturing aspects, the most suitable region to increase the interwinding space is the external part (region 2 of Fig. 3). Therefore, in this paper, only the external interwinding space of the toroidal transformer is used to increase the leakage inductance; see Fig. 5. Taking this into consideration, the leakage inductance for the vertical external component of the winding (region 2), given by (8), is modified as follows:

$$L'_{leak,2} = \frac{N^2 \mu_0 h}{2\pi} \left[\left(\frac{R_{m5}}{R_6^2} \right) \frac{b}{3} + \left(\frac{1}{2R_e(R_7 + \Delta g)} \right) \left(R_{m6} + \frac{\Delta g}{2} \right) (g + \Delta g) + \left(\frac{R_{m7} + \Delta g}{R_7^2} \right) \frac{a}{3} \right] \quad (18)$$

where Δg is the increased space in the interwinding region. The leakage inductance corresponding to the horizontal components of the winding (regions 3 and 4), given by (12), is also modified, resulting in the following expression:

$$L'_{leak,3} = \frac{N^2 \mu_0 \left[(R_e + \Delta g)^2 - R_i^2 \right]}{2\pi (R_e + \Delta g) R_i} \left(\frac{b}{3} + g + \frac{a}{3} \right). \quad (19)$$

Fig. 6(a) shows the variation of the leakage inductance with the interwinding space for the four transformer ratings under study. One can appreciate that increasing the interwinding spacing increases the leakage inductance by a relatively modest amount. The values have been normalized with respect to the minimum interwinding space needed for insulation purposes (1 mm).

The results from the formulas of this paper against FEM are compared in Fig. 6(b) for the transformer 25 kVA. One can appreciate a very good match between the formulas and FEM (differences of about 4%).

As a conclusion of this section, one can observe that the technique of increasing interwinding spacing is effective when relatively small increments of the leakage inductance are needed. However, when large increments are sought, a different technique is necessary. Furthermore, adding larger spaces than required for insulation purposes adds cost and weight to the transformer. The most significant negative consequence is that the

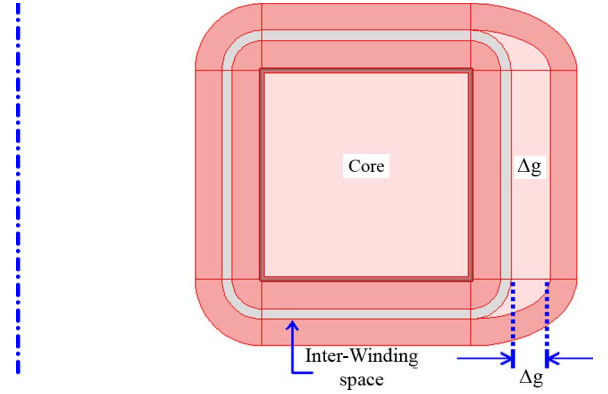


Fig. 5. Enlarging the external vertical interwinding space to augment the leakage inductance.

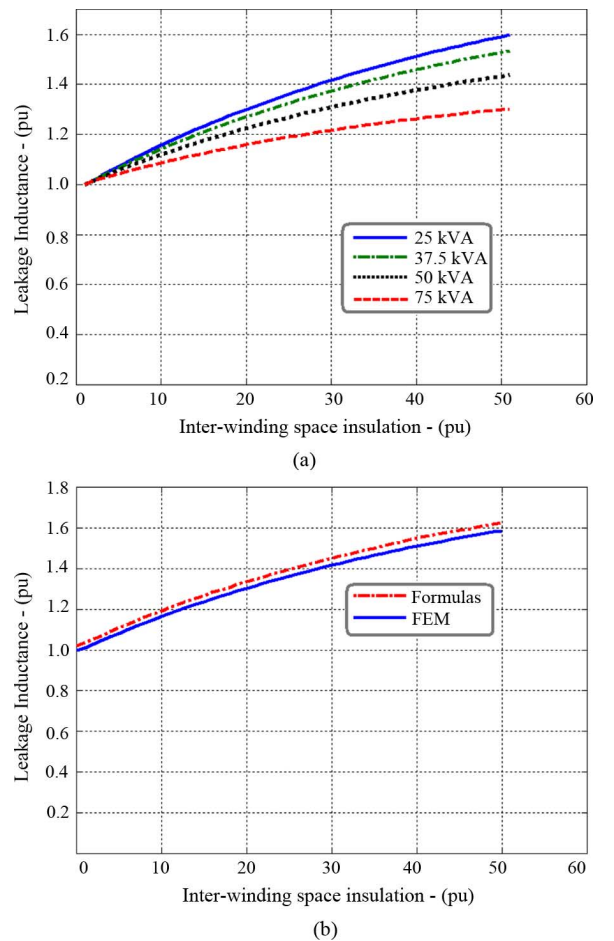


Fig. 6. Variation of the leakage inductance: (a) Calculated for four different ratings of toroidal distribution transformers. (b) Comparison of the analytical results with FEM for a 25-kVA toroidal transformer.

external winding has a longer mean length (adding production cost and operation losses).

B. Ferromagnetic Inserts

The second technique proposed in this paper to increase the leakage inductance is to augment the permeability of the material in the leakage region. By inserting ferromagnetic material

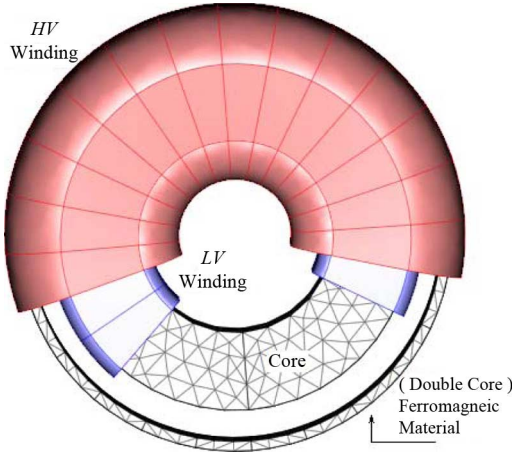


Fig. 7. Illustration of adding ferromagnetic inserts between windings to increase the leakage inductance.

between the windings, we can dramatically magnify the leakage inductance without a noticeable increase in the transformer size.

The underlying idea is to install a thin core in the interwinding region on the external face; see Fig. 7. This produces an enlargement of the leakage inductance component corresponding to such a region. Equation (8) is modified as

$$L'_{\text{leak},2} = \frac{N^2 \mu_0 h}{2\pi} \left[\begin{aligned} & \left(\frac{R_{m5}}{R_6^2} \right) \frac{R_{m5} b}{3} + \\ & \left(\frac{1}{2R_6(R_7 + g_c)} \right) (R_{m6} + \frac{g_c}{2}) (g + \mu_r g_c) \\ & + \left(\frac{R_{m7} + g_c}{R_7^2} \right) \frac{a}{3} \end{aligned} \right] \quad (20)$$

where g_c is the thickness of the region occupied by the ferromagnetic material and μ_r is its relative permeability. The leakage inductance for the horizontal components of the winding is modified in a similar fashion as (12), yielding:

$$L_{\text{leak},3} = \frac{N^2 \mu_0 \left[(R_e + g_c)^2 - R_i^2 \right]}{2\pi (R_e + g_c) R_i} \left(\frac{b}{3} + g + \frac{a}{3} \right). \quad (21)$$

By adding material with high relative permeability (μ_r), the value of the leakage inductance can be magnified by a large factor. When using this technique, care must be taken to avoid saturation of the thin core placed between the windings.

Different ferromagnetic materials [15] were considered for the simulations performed to validate this technique. Fig. 8(a) shows the variation of leakage inductance with thickness for materials with different permeability. The plot is given in per unit (p.u.), normalized to the minimum insulation space and permeability of air μ_0 . A comparison between the results of the formulation and FEM is shown in Fig. 8(b). One can notice that the differences are very small.

VI. EXPERIMENTAL VERIFICATION

With the purpose of validating the formulas proposed in this paper and the FEM simulations, a set of prototypes was built with ratings of 150 VA, 300 VA, 1 kVA, 2 kVA, and 4 kVA. The leakage inductance was measured by applying two methods: 1) using the standardized short-circuit (SC) test and 2) using

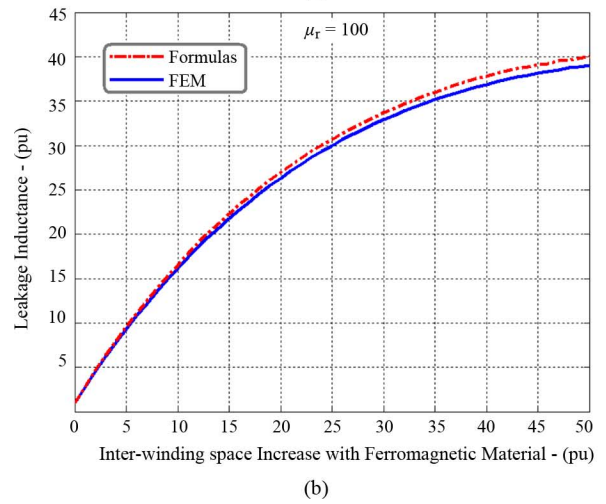
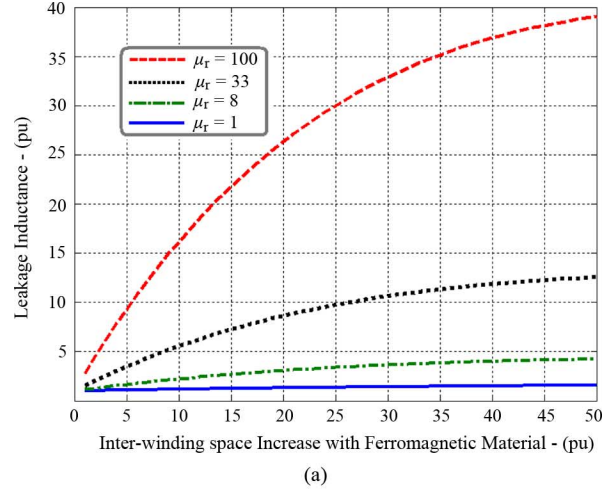


Fig. 8. Increase of the leakage inductance. (a) Inserting four different ferromagnetic materials between the windings. (b) Comparison of results between formulas and FEM for the 25-kVA transformer.

an RLC meter (7600 Precision LCR meter) available in the lab. This meter uses an ac signal of 2 V at 60 Hz and it gives the equivalent series R-L circuit of the transformer directly. In all cases, the secondary windings of the transformers are shorted and the primary windings are connected to the source.

Table V shows the comparison of the measurements on the five prototypes against finite elements simulations and the formulas of this paper. One can appreciate that for most cases, the results are very close between the four different methods (SC, RLC meter, FEM, and formulas). The differences are, in general, less than 3%. The sole exception is the SC measurement of the 300-VA double-core transformer with 8.47% difference. This transformer was opened and unwound. We found that the external (powder) core was fractured. Therefore, the effective permeability of this core was reduced by the irregular (unintended) air gap, explaining why the measurements gave a slightly smaller leakage inductance when compared with FEM and the formulas.

These experiments not only corroborate the accuracy of the calculation method proposed in this paper, but also confirm the applicability of ferromagnetic inserts to increase the leakage inductance when large leakage is necessary.

TABLE V
LEAKAGE INDUCTANCE MEASURED AND COMPUTED
FOR SINGLE-PHASE TOROIDAL TRANSFORMERS

Transformer	Leakage Inductance		Leakage Inductance		% Diff SC versus Formula
	Measured (mH)		Computed (mH)		
	SC	RLC	FEM	Formula	
150 VA	0.7200	0.7350	0.6890	0.7095	1.46
1 kVA	0.2150	0.2300	0.2100	0.2092	2.68
2 kVA	0.0493	0.0491	0.0490	0.0503	2.03
4 kVA	0.0209	0.0220	0.0205	0.0205	1.53
*300 VA	13.644	**	15.100	14.800	8.47

* Transformer with double core (as in Fig. 7)

** Not possible to measure with the RLC meter

VII. CONCLUSION

Formulas suitable for a design program for the calculation of the leakage inductance of toroidal transformers have been developed. From the observation of the distribution of the magnetic flux in the leakage region, precise expressions have been derived for the magnetic-field strength. The leakage inductance is obtained by the analytical integration of the total energy stored in the magnetic field. The formulas have been compared against 2-D and 3-D finite-element simulations, yielding very good results; with differences under 4%.

Two methodologies to augment the leakage inductance of toroidal transformers have been proposed. We have investigated increasing the interwinding spacing and the addition of a ferromagnetic core in the leakage region. Increasing the interwinding spacing is effective for up to a 1.5-p.u. increment of the leakage inductance at the cost of increasing the mean length of the external winding. The addition of a ferromagnetic core between the windings offers an inexpensive alternative to augment the leakage inductance. This technique can be conveniently used to increase the leakage inductance of several orders of magnitude.

The accuracy of the formulas and the applicability of the methods to increase the leakage inductance have been corroborated experimentally for a set of prototypes of various sizes.

ACKNOWLEDGMENT

The authors would like to thank U. Poulsen of Bridgeport Magnetics for his fast response and expertise building the prototypes. The authors would also like to thank C. Prabhu and N. Augustine, M.Sc. students of Polytechnic Institute of New York University, for performing the leakage inductance tests to the prototypes. In addition, the authors would like to thank the reviewers for their sharp comments that have added value to this paper.

REFERENCES

- [1] F. A. Furfari and J. W. Coltman, "The transformer," *IEEE Ind. Appl. Mag.*, vol. 8, no. 1, pp. 8–15, Jan./Feb. 2002.
- [2] S. Jeszensky, "History of transformers," *IEEE Power Eng. Rev.*, vol. 16, no. 12, pp. 9–12, Dec. 1996.
- [3] J. H. Harlow, *Electric Power Transformer Engineering*, 2nd ed. Boca Raton, FL: CRC, 2007.
- [4] S. V. Kulkarni and S. A. Khaparde, *Transformer Engineering Design and Practice*. New York: Marcel Dekker, 2004.

- [5] R. M. V. Del, B. Poulin, P. T. Feghali, D. M. Shah, and R. Ahuja, *Transformer Design Principles—With Application to Core-Form Power Transformers*. New York: Gordon and Breach, 2001.
- [6] M. Heathcote, *J & P Transformer Book*, 12th ed. London, U.K.: Butterworth-Heinemann, 1998.
- [7] M. van der Veen, *Modern High-end Valve Amplifiers: Based on Toroidal Output Transformers*. Dorchester, U.K.: Elektor Electronics Publishing, 1999.
- [8] A. A. Halacsy, "Reactance and eddy current loss in toroidal transformer devices-II," *AIEE Trans. Power App. Syst.*, vol. 81, no. 3, pp. 1017–1019, Apr. 1962.
- [9] R. Prieto, J. A. Cobos, V. Bataller, O. Garcia, and J. Uceda, "Study of toroidal transformers by means of 2D approaches," presented at the IEEE 28th Ann. Power Electron. Specialists Conf., St. Louis, MO, Jun. 22–27, 1997.
- [10] R. Prieto, V. Bataller, J. A. Cobos, and J. Uceda, "Influence of the winding strategy in toroidal transformers," in *Proc. IEEE 24th Annu. Conf. Ind. Electron. Soc.*, Sep. 1998, vol. 1, pp. 359–364.
- [11] J. P. Myers, K. A. Weaver, W. R. Wieserman, and U. Poulsen, "O cores—A new approach," in *Proc. Elect. Insul. Conf. Elect. Manuf. Coil Winding Technol. Conf.*, Sep. 23–25, 2003, pp. 193–198.
- [12] P. Gómez, F. d. León, and I. Hernández, "Impulse response analysis of toroidal core distribution transformers for dielectric design," *IEEE Trans. Power Del.*, vol. 26, no. 2, pp. 1231–1238, Apr. 2011.
- [13] *IEEE Recommended Practice for Protection and Coordination of Industrial and Commercial Power Systems*, IEEE Std. 242-1986, Feb. 1986.
- [14] "Comsol Multiphysics, AC/DC User's Guid," Comsol AB Group, 2006, pp. 1–156.
- [15] A. Goldman, *Handbook of Modern Ferromagnetic Materials*. Norwell, MA: Kluwer, 1999, vol. I, pp. 64–135.

Iván Hernández (S'06) was born in Salamanca, Guanajuato, Mexico, in 1979. He received the B.Sc. degree in electrical engineering from the University of Guanajuato, Salamanca, Guanajuato, Mexico, in 2002, and the M.Sc. degree in electrical engineering from the CINVESTAV Guadalajara, Jalisco, Mexico, in 2005, where he is currently pursuing the Ph.D. degree.

From 2008 to 2010, he was on a study leave at the Polytechnic Institute of New York University, Brooklyn, NY. Previously, he was an Electrical Engineer Designer for two years with FMS Ingeniería, Guadalajara, Mexico. His research interests are numerical analysis applied to machine design and software simulation tools, particularly for electromagnetic fields.

Francisco de León (S'86–M'92–SM'02) was born in Mexico City, Mexico, in 1959. He received the B.Sc. and the M.Sc. degrees in electrical engineering from the National Polytechnic Institute, Mexico City, Mexico, in 1983 and 1986, respectively, and the Ph.D. degree from the University of Toronto, Toronto, ON, Canada, in 1992.

He has held several academic positions in Mexico and has worked for the Canadian electric industry. Currently, he is an Associate Professor at the Polytechnic Institute of New York University, Brooklyn, NY. His research interests include the analysis of power phenomena under nonsinusoidal conditions, the transient and steady-state analyses of power systems, the thermal rating of cables, and the calculation of electromagnetic fields applied to machine design and modeling.

Pablo Gómez (S'01–M'07) was born in Zapopan, México, in 1978. He received the B.Sc. degree in mechanical and electrical engineering from Universidad Autónoma de Coahuila, Mexico, in 1999, and the M.Sc. and Ph.D. degrees in electrical engineering from CINVESTAV, Guadalajara, Mexico, in 2002 and 2005, respectively.

Since 2005, he has been a Full-Time Professor with the Electrical Engineering Department, SEPI-ESIME Zacatenco, National Polytechnic Institute, Mexico City, Mexico. From 2008 to 2010, he was on a postdoctoral leave at the Polytechnic Institute of New York University, Brooklyn, NY. His research interests are modeling and simulation for electromagnetic transient analysis and electromagnetic compatibility.